CEA Comité Español de Automática
XLVII JORNADAS DE AUTOMÁTICA CÓRDOBA 2026
UNIVERSIDADE DA CORUÑA

Jornadas de Automática

Characterizing 3D-printed soft joints: material, temperature, and infill density analysis

Jaime González-Menocal[a,*], Emilia Adela Laber[b], Claudia Sánchez[a], Lisbeth Mena[a], Jorge Muñoz[a], Concepción A. Monje[a]

[a]*RoboticsLab, Departamento de Ingeniería de Sistemas y Automática, Universidad Carlos III de Madrid, Avenida de la Universidad 30, 28911 Leganés, Madrid, España.*
[b]*University of Applied Sciences Technikum Wien, Höchstädtpl 6, 1200 Viena, Austria.*

To cite this article: González-Menocal, J., Laber, E.A., Sánchez, C., Mena, L., Muñoz, J., Monje, C.A. 2026. Characterizing 3D-printed soft joints: material, temperature, and infill density analysis. Jornadas de Automática, 47. https://doi.org/10.17979/ja-cea.2026.47.13775

Abstract

This paper presents the mechanical characterization of tendon-driven, multi-segment soft joints fabricated via Fused Deposition Modeling (FDM), exploring internal infill density and active thermal foaming as primary tuning parameters. We systematically evaluate joints printed with varioShore TPU—a foaming elastomer—across a thermal gradient and varying porous infill densities, comparing the results against a standard Filaflex 82A baseline. Tensile tests reveal that modulating infill density provides a predictable, non-linear amplification of structural stiffness. Furthermore, thermal activation of the foaming agent in varioShore TPU drastically enhances mechanical resistance. Compared to Filaflex, the foamed varioShore achieves superior absolute strength and a vastly broader tunable bandwidth. These findings demonstrate that active foaming filaments offer great versatility and provide a baseline for designers to program both delicate compliance and high rigidity from a single material.

Keywords: Soft robotics, Smart structures and vibration control, Mechatronic system modeling, design, optimization, Advanced manufacturing and remanufacturing technologies, Robotic grasping and manipulation.

Caracterización de articulaciones blandas impresas en 3D: análisis de material, temperatura y densidad de relleno.

Resumen

Este artículo presenta la caracterización mecánica de articulaciones blandas accionadas por tendones y fabricadas mediante Modelado por Deposición Fundida (FDM), explorando la densidad de relleno interno y la espumación térmica activa como parámetros principales de ajuste. Se evalúan articulaciones blandas impresas con varioShore TPU, un elastómero espumante, variando la temperatura y las densidades de relleno, comparando los resultados frente a un TPU estándar de referencia de Filaflex 82A. Los ensayos de tracción revelan que aumentar la densidad de relleno proporciona una amplificación predecible y no lineal de la rigidez estructural. Además, la activación térmica del agente espumante en el varioShore TPU mejora la resistencia mecánica. En comparación con Filaflex, el varioShore espumado alcanza una resistencia superior y un rango de ajuste mucho más amplio. Este artículo demuestra que los filamentos de espumación activa ofrecen versatilidad y proporciona una base que permite a los diseñadores programar las mismas articulaciones con diferentes propiedades a partir de un único material.

Palabras clave: Robótica blanda, Estructuras inteligentes y control de vibraciones, Modelado, diseño y optimización de sistemas mecatrónicos, Tecnologías avanzadas de fabricación y refabricación, Agarre y manipulación robótica.

1. Introduction

The evolution of robotics has increasingly modified from rigid, high-stiffness mechanisms toward soft and compliant systems capable of safer and more adaptive interaction with humans, objects, and unstructured environments. This transition is particularly relevant in applications such as healthcare, human-robot collaboration, wearable devices, and the manip-

*Autor para correspondencia: jgmenoca@ing.uc3m.es

ulation of fragile objects, where mechanical compliance can reduce injury risks and improve the ability of robots to adapt to uncertain geometries (Yasa et al., 2023). While traditional rigid robots offer high precision, speed, and load capacity, their fixed geometry and inherent stiffness can make physical interaction hazardous and limit their performance in delicate, or deformable environments. In contrast, soft robots can deform under external loads, absorb impacts, distribute contact forces, and adapt their shape to the surrounding environment, enabling functions such as grasping irregular objects, navigating confined spaces, assisting surgical and rehabilitation tasks, and interacting more naturally with biological tissue (Wang et al., 2024).

Within this context, Fused Deposition Modeling (FDM) has emerged as a key manufacturing technology for the rapid prototyping of soft robotic components. Its low cost, accessibility, and compatibility with CAD design workflows make it particularly suitable for the iterative development of geometrically complex structures. In soft robotics, FDM enables the exploration of wall thicknesses, infill patterns, curvatures, lattice structures, internal channels, and hybrid architectures that combine flexible and rigid regions. This capability is especially valuable when designing adaptive components whose mechanical response depends not only on the material itself but also on the printed architecture (Rodríguez-Sanz et al., 2025). Recent studies have highlighted the potential of extrusion-based additive manufacturing for producing customized soft devices with high functional complexity, as well as multimaterial components with flexible regions, embedded elements, and enhanced impact absorption (Henríquez et al., 2024).

Despite these advantages, the design freedom offered by FDM is accompanied by significant mechanical uncertainty. The final performance of printed parts depends strongly on process-related variables such as print path, raster orientation, layer adhesion, void formation, infill density, and thermal history. As a result, the geometry of an FDM-printed component is often easier to control than its final mechanical response. Even when using well-established flexible filaments such as thermoplastic polyurethane (TPU), the resulting stiffness, damping, deformation behavior, and failure limits may vary considerably depending on the selected printing parameters. This has motivated the development of process-to-property approaches for FDM polymers, in which the printed material response is understood as the result of both the base resin and the manufacturing conditions (Garzon-Hernandez et al., 2020; Gallup et al., 2024). In general, FDM remains a complex process in which a large number of parameters affect the quality, repeatability, and mechanical properties of the manufactured components (Chacón et al., 2017).

This uncertainty becomes even more pronounced with the introduction of newer active foaming materials, whose properties can be modified through the printing process itself. Unlike conventional flexible filaments, these materials can expand or change their internal structure as a function of parameters such as printing temperature, thereby altering density, stiffness, and deformation behavior.

Although this tunability offers opportunities for lightweight and functionally graded soft robotic structures, it also increases the difficulty of predicting the final mechanical response of printed actuators. In tendon-actuated soft joints, this uncertainty is particularly relevant because printing temperature, material selection, and infill density directly affect the force that the joint is able to withstand. However, these relationships remain insufficiently mapped, especially for materials whose properties are strongly dependent on the printing process.

The present work addresses this gap through a mechanical characterization of FDM-printed tendon-actuated soft joints, using a soft actuator as a representative case study. This actuator presents a complex response due to its deformation and directional locking behavior, where the resulting performance depends on the interaction between material compliance, internal architecture, printing parameters, and tendon-driven loading. By comparing a conventional flexible filament with a thermo-responsive active foaming material under different infill densities and printing temperatures, this study evaluates how these variables influence the force levels achievable in the soft joint. The main contribution of this work is the translation of mechanical characterization results into a design guide for printed soft joints. By relating material selection, printing temperature, and infill density to the force required at the joint, the proposed dataset provides a basis for choosing manufacturing parameters. This reduces reliance on an empirical design approach based on Trial and error and encourages the development of soft robotic actuators with more accurate prediction capabilities.

The structure of the paper is as follows: the materials and methods are presented in Section 2, the experimental results are compiled in Section 3, the discussion is in Section 4, and finally, Section 5 presents the conclusions.

2. Materials and Methods

2.1. FDM Soft Filaments and Active Foaming Technology

This work focuses on temperature as one of the three main parameters of study. Therefore, both a constant-density filament and a temperature-dependant filament are used. These filaments are Recreus Filaflex 82A and ColorFabb varioShore Prosthetic. Filaflex is a commercially available TPU filament with a shore hardness of 82A that exhibits stable mechanical properties independent of extrusion temperature variations. VarioShore is also a TPU filament with Active Foaming Technology (AFT). VarioShore incorporates a chemical blowing agent that triggers at elevated temperatures. When extruded between 200ºC and 230ºC, the material experiences foaming, reducing its density and altering its effective Shore hardness. This allows for the ”programming” of local structural stiffness through temperature changes during the printing process.

Table 1: Material specifications for the selected flexible FDM filaments.

Technical Specification	Filaflex	varioShore
Nominal Density [g/cm^3]	1.12	1.20
Base Hardness [Shore A]	85A	92*
Young's Modulus [MPa]	22	59*
Tensile Strength [MPa]	45	24*
Elongation at Break	650%	465%*
Nozzle Temperature [°C]	230 - 248	195 - 260

* *Note: varioShore values represent unfoamed baseline properties.*

2.2. Soft Joint Morphology and Design

The soft joint used for the experiments in this work is based on a continuum soft-robotic arm design (Relaño et al., 2023). This joint is actuated through tendons that allow for the inclination of the soft structure, providing two degrees of freedom (DoF): orientation and inclination. Structurally, the joint consists of a series of stacked triangular sections that are joined at the center by a cylindrical column; these stacked sections are referred to as soft links. At the vertices of these triangular sections, three channels are positioned at 120° intervals to allocate the actuation tendons (Monje et al., 2024). A representation of the soft joint and its geometry can be found in Figure 1.

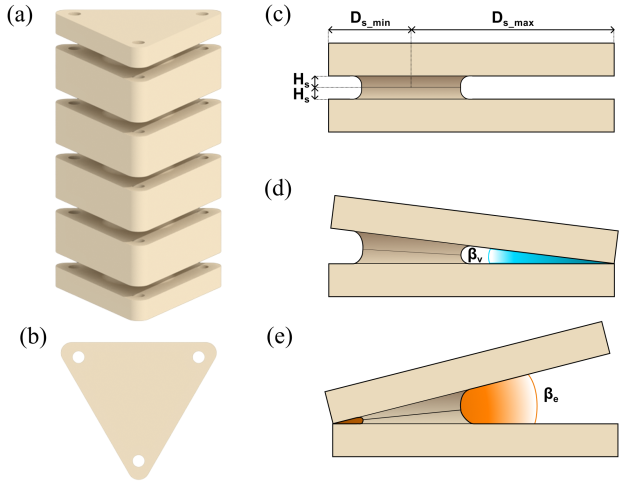

Figure 1: Geometric architecture and contact limits of the soft joint: (a) 3D model perspective of the stacked soft link structure; (b) top cross-section view illustrating the 120° tendon channel alignment; (c) profile view schematic defining section height (H_s), edge-blocking distance ($D_{s\_\min}$), and vertex-blocking distance ($D_{s\_\max}$); (d) single-tendon vertex-blocking limit state highlighting angle β_v; and (e) dual-tendon edge-blocking limit state highlighting the wider angle β_e.

These soft links feature a geometry-induced blocking mechanism, meaning that as the joint bends and adjacent sections of the link come into contact, the local curvature is limited and further bending is mechanically restricted. Depending on the specific actuation of the tendons, two distinct blocking configurations arise:

1. Vertex Blocking: When actuating a single tendon, the joint bends toward a vertex. The distance at which contact occurs is defined as the maximum clearance distance $D_{s\_\max}$, and the corresponding maximum bending limit is denoted as the vertex blocking angle β_v.
2. Edge Blocking: Conversely, when actuating two tendons simultaneously, the joint bends toward a flat edge. In this configuration, the adjacent sections collide much sooner at a minimum clearance distance defined as $D_{s\_\min}$. This yields an edge blocking angle β_e, which is inherently greater than the vertex blocking angle ($\beta_e > \beta_v$).

These blocking angles are directly dependent on the distance between the center of the cylindrical column and the flat edge of the triangular section, known as the section height H_s. This geometric parameter fundamentally dictates the displacement required to achieve these blocking states. Consequently, the mechanical limits and the resulting bending workspace of the soft joint are inherently anisotropic and fully governed by this cross-sectional geometry.

2.3. Specimen Fabrication and Printing Strategy

While the soft joint architecture inherently possesses two distinct blocking orientations depending on the actuation paths, the experimental characterization trials conducted in this work focus exclusively on evaluating the joint's structural behavior under vertex-blocking configurations. This choice isolates a consistent deformation axis to analyze the printing parameter variances directly against a singular geometric baseline limit. For all fabricated test specimens, the core structural proportions and macro-dimensions were held constant across both material batches. Each specimen features a total nominal structural length of 50 mm, comprising an assembly of exactly 5 stacked soft links, with an individual section height (H_s) of 1.3 mm. Based on these defined parameters, the theoretical maximum vertex-blocking angle (β_v) for this specific multi-segment assembly is geometrically fixed at 7.12°. These localized geometric constants and structural constraints are systematically summarized in Table 2.

Table 2: Fixed geometric parameters of the evaluated soft joint specimens.

Geometric Parameter	**Value**
Total Length [mm]	50
Number of links	5
Section Height (H_s) [mm]	1.30
Vertex Blocking Angle (β_v) [°]	7.12

To analyze how manufacturing variations influence the structural response of the joint, a multi-variable factorial characterization matrix was established. This experimental design evaluates three primary process parameters across a total of 5 combinations: 2 base material formulations (Recreus Filaflex 82A and colorFabb varioShore Prosthetic TPU), 4 extrusion temperatures (200°C, 210°C, 220°C, and 230°C), and 6 infill densities. The density steps range from 10% to 90% in 20% increments (10%, 30%, 50%, 70%, and 90%) using an isotropic gyroid pattern, alongside an additional 100% solid configuration using a rectilinear pattern (see Figure 2). The total number of physical specimens printed for this study is derived from the combinations within this factorial design. While Filaflex serves as the geometric control group printed at a single optimized temperature (230°C), the varioShore material is swept across all 4 target temperatures to map the active foaming profiles. This yields a total of 30 unique manufacturing configurations. To ensure statistical traceability and guarantee manufacturing process repeatability, exactly 3 distinct physical specimens were 3D printed for every individual configuration. Consequently, the total number of physical specimens manufactured and evaluated is 90. Furthermore, because each individual specimen was subsequently subjected to 3 consecutive mechanical testing repetitions to capture steady-state signatures, the complete experimental dataset encompasses $N = 270$ individual trial runs. This highly robust data pool allows for an accurate calculation of the statistical mean and standard deviation (σ) across all parameter boundaries.

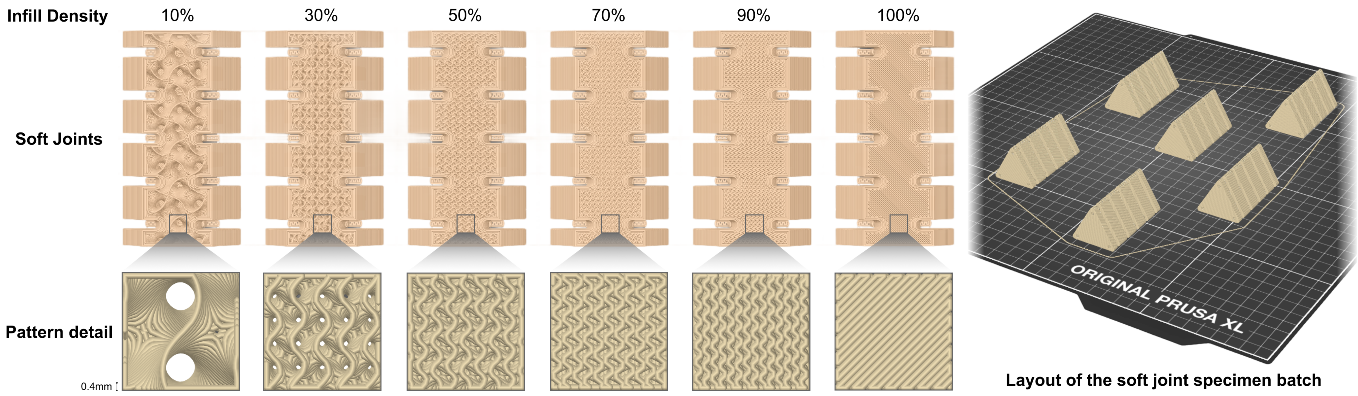

Figure 2: Internal macro-morphology and structural gradients of the 3D-printed soft link segments across the evaluated infill density spectrum (ranging from low-density internal compliance to a fully solid cross-section).

2.4. Experimental Setup and Characterization Protocol

Mechanical characterization was conducted using a calibrated universal testing machine (INSTRON) equipped with a precise electronic load cell to capture the force-displacement profile of each joint configuration. This assembly and procedure is based on the set-up presented by Sánchez et al. (2026) and the complete experimental assembly is illustrated in Figure 3.

To isolate the vertex-blocking structural compliance, each 3D-printed soft joint specimen was fixed vertically inside the machine's testing chamber. The bottom base of the joint was anchored to the lower static platform of the frame, preventing any translation or parasitic rotations at the root. The internal actuation tendon corresponding to the target vertex axis was routed through the joint channels and extended vertically from the top link segment. This tendon terminal was securely clamped into the upper mechanical grip attached directly to the moving crosshead load cell.

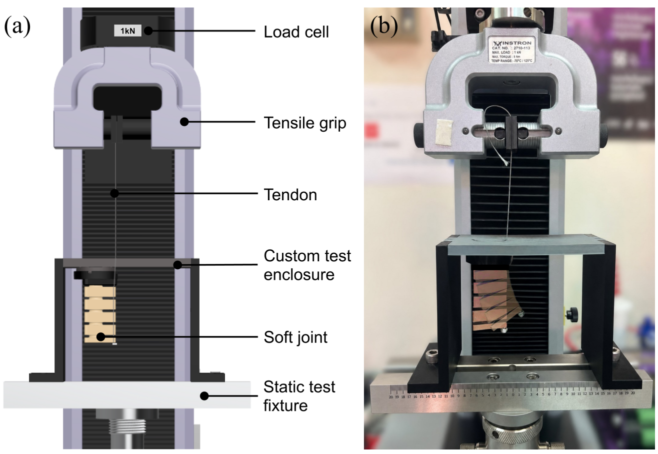

Figure 3: Experimental test configuration mounted inside a rigid protective enclosure: a multi-segment soft joint specimen rigidly anchored at the static base platform while an isolated actuation tendon is tensioned vertically by the upper mechanical crosshead grip.

The characterization protocol was executed under quasi-static, displacement-controlled conditions. The upper tensile gripper moved upward at a constant velocity of 40mm/min, tensioning the tendon and forcing the multi-segment joint to transition from its straight rest state into a progressive flexural curve until the vertex-blocking limit was fully engaged. Data logging captured the tensile force response against the absolute vertical displacement of the crosshead at a sampling frequency of 50 Hz. Each unique configuration was tested using 3 distinct physical specimens, with each specimen undergoing 3 consecutive loading cycles to guarantee data repeatability. To allow for the elastic recovery of the specimens, each of the cycles were separated by 5 minute intervals. The maximum travel limit was set to 12 mm to ensure that the physical contact state was engaged. The definitive vertex-blocking threshold used to evaluate and compare the structural variations was numerically isolated at a theoretical displacement of 12 mm utilizing a custom MATLAB post-processing script. This script outputs the measured linear tendon displacement directly to the joint's effective bending angle by evaluating the inverse kinematics equations parameterized with the nominal design dimensions. The fixed operational parameters of the testing setup are summarized in Table 3.

Table 3: Operational parameters for the quasi-static mechanical characterization protocol.

Testing Parameter	Value / Condition
Displacement Rate [mm/min]	40
Sampling Rate [Hz]	50
Maximum Displacement [mm]	12
Evaluation Displacement [mm]	10
Replications per Specimen	3

3. Results

3.1. General Mechanical Behavior

During the tensile characterization conducted on the INSTRON testing system, the soft joints exhibited a highly consistent and progressive bending response under tendon-driven tension. Initially, the joints rested in a straight, unconstrained configuration. As the machine applied displacement (δ), the tendon force induced continuous flexure across the soft joint. This progressive deformation continued until structural locking occurred.

To illustrate the fundamental mechanical signature of the design, Figure 4 presents a force-displacement curve of the joint over three consecutive cycles. The signature highlights the inherent elastic nature of the material. During the initial loading phase, the structure undergoes a primary settling period characterized by minor stress relaxation and hysteresis. However, in subsequent cycles, the joint demonstrates excellent mechanical repeatability.

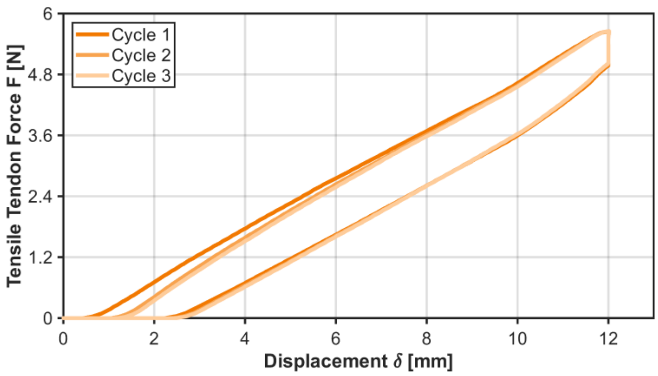

Figure 4: Force-displacement example of three cycles of a specimen.

3.2. *Influence of Infill Density on Maximum Force*

Internal infill density serves as the primary parameter for mechanical tunability. As detailed in Table 4 and Figure 5, increasing the infill percentage drives a predictable, non-linear amplification in peak tensile force. Low-density configurations (10%–30%) exhibit highly compliant behavior, requiring minimal force to achieve full flexure. Conversely, structural stiffness increases dramatically approaching solid infill.

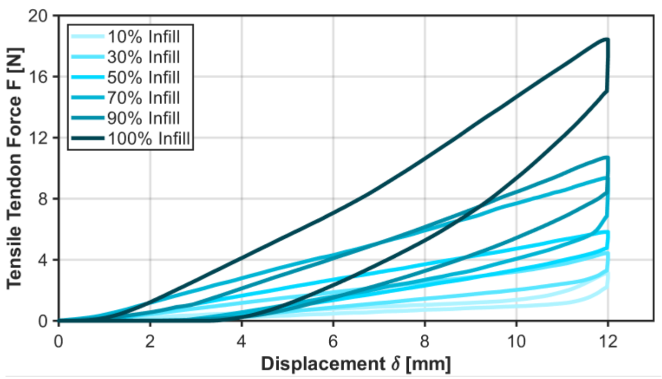

Figure 5: Peak tensile force plotted as a function of infill density across the experimental batches.

3.3. *Thermal Effects on varioShore Performance*

The active foaming agent in varioShore TPU provides a secondary, thermally driven tuning mechanism. Evaluating four temperature batches for the same material shows a substantial gain in required actuation force as extrusion temperature rises. Higher temperatures amplify gas expansion, effectively thickening the joint's internal struts and resisting compression more aggressively.

This impact is most evident at 100% infill: the baseline unfoamed samples (200°C) required a peak force of 11.394 ± 3.475 N. This value progressively scales to 13.394 ± 1.666 N (210°C), 16.548 ± 2.455 N (220°C), and ultimately 23.919 ± 1.885 N (230°C). This represents a 110% increase in structural stiffness driven entirely by thermal activation, without altering the slicer density profile.

The data collected for each of the configurations was averaged and used to create a fitted curve that works as a force-infill function. This provides a reliable guide on the effect of temperature on the behavior of a soft joint printed with varioShore TPU. All of this data is best represented in Figure 6.

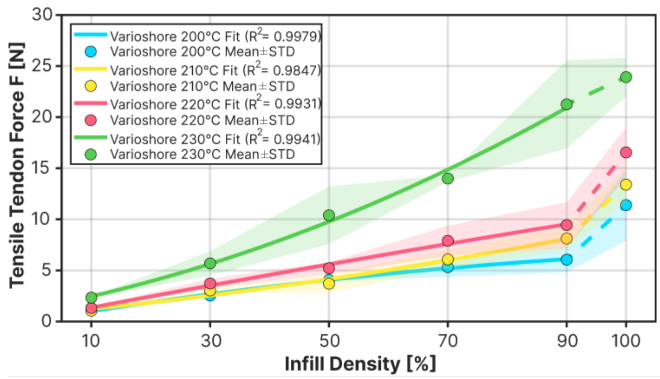

Figure 6: Comparative force-displacement profiles across four thermal batches of varioShore TPU. Continuous lines represent the fitted-curve function, whereas the dashed lines represent an approximation of the real behavior, due to differences in infill pattern.

3.4. *Material Comparison: varioShore vs. Filaflex 82A*

To contextualize the active foaming structure, the maximally foamed varioShore (230°C) was compared against a standard Filaflex 82A baseline printed at the same temperature. Figure 7 demonstrates that varioShore significantly outperforms Filaflex in both absolute strength and functional versatility.

At 100% solid density, the foamed varioShore structure provides superior rigidity. More critically for soft robotic applications, varioShore offers a vastly broader tunable range. While Filaflex scales from roughly 0.96 N to 13.64 N, the varioShore batches span from 1 N to nearly 24 N.

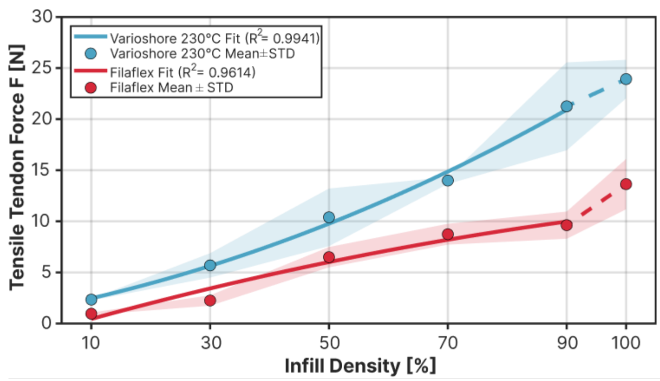

Figure 7: Comparative force-infill profiles of varioShore TPU and Filaflex 82A both printed at 230°C.

Table 4: Mean force values and standard deviations by material type, printing temperature, and infill density.

Material and temperature	**Infill Density**					
	10%	30%	50%	70%	90%	100%
VS - 200ºC	1.074 ± 0.118	2.544 ± 0.235	4.083 ± 0.122	5.320 ± 0.958	6.049 ± 1.244	11.394 ± 3.475
VS - 210ºC	1.058 ± 0.083	3.040 ± 0.209	3.709 ± 0.916	6.084 ± 0.933	8.124 ± 1.094	13.394 ± 1.666
VS - 220ºC	1.324 ± 0.091	3.726 ± 0.476	5.212 ± 0.585	7.894 ± 1.491	9.437 ± 2.224	16.548 ± 2.455
VS - 230ºC	2.340 ± 0.077	5.688 ± 1.193	10.393 ± 2.816	13.994 ± 0.333	21.253 ± 4.302	23.919 ± 1.885
FF - 230ºC	0.958 ± 0.110	2.251 ± 0.509	6.493 ± 0.993	8.740 ± 1.019	9.625 ± 1.329	13.639 ± 2.462

4. Discussion

The range of varioShore TPU allows for the customization of soft robotic for different applications. Configurations requiring minimal actuation force exhibit high compliance and rapid flexibility, ideal for delicate manipulation tasks, while configurations with high infill density are better suited for greater payload applications, such as soft robotic joints in humanoid robots.

When analyzing the structural transition toward maximum density, it is crucial to account for a topological discontinuity at 100% infill. While intermediate densities rely on procedurally generated porous internal structures due to the gyroid pattern, the 100% configuration defaults to a solid rectilinear in the slicer software. This geometric shift alters the internal load distribution and stress propagation within the joint. Consequently, the mechanical jump observed between the 90% and 100% specimens is not solely a function of increased polymeric mass, but also a direct result of this internal pattern transition. Designers must explicitly factor this topological change into the predictive modeling of fully solid components.

Future research will focus on expanding this characterization framework to explore other printing parameter variations, such as varied print speeds, and non-standard layer heights to push the limits of the foaming agent. Additionally, it is necessary to investigate a wider array of soft joint morphologies, from scaling this design to new sets of parameter configurations. By altering bending angles, section heights, and introducing multi-tendon bending geometries at the edge of the joint, it is possible to develop a comprehensive predictive design library for FDM-printed soft actuators. Furthermore, since these tests were restricted to quasi-static conditions, dynamic characterization and long-term fatigue testing remain pending for future research.

5. Conclusions

This study demonstrates that FDM, combined with active foaming elastomers like varioShore TPU, provides a highly effective method for tuning the mechanical properties of soft robotic joints. By systematically modulating internal infill density and extrusion temperature, we achieved predictable, non-linear control over structural stiffness.

The thermal activation of the foaming agent proved particularly impactful, successfully increasing the mechanical resistance of the joints at maximum density, completely independent of the external geometry. Furthermore, the foamed varioShore TPU outperformed the standard baseline, with both superior absolute peak force and a significantly broader tunable range. These findings allow designers to seamlessly integrate both delicate compliance and robust rigidity into soft robotic systems using a single continuous material.

Acknowledgments

The research leading to these results has been supported by the ADAPTA project, with reference PLEC2023-010218, funded by MICIU/AEI/10.13039/501100011033, the SIROCO project, with reference PID2023-147343OB-I00, funded by MICIU/AEI/10.13039/501100011033 and FEDER, UE, the AdaptativeFold project of the Early Career Researchers Grant Program with reference number 2025/00832/001, and the Early Career Researchers Grant Program with reference number 2025/00764/001, both awarded by the Carlos III University of Madrid as part of the UC3M's own research program.

References

Chacón, J., Caminero, M., García-Plaza, E., Núñez, P., 2017. Additive manufacturing of PLA structures using fused deposition modelling: Effect of process parameters on mechanical properties and their optimal selection. Materials Design 124, 143–157.
DOI: `https://doi.org/10.1016/j.matdes.2017.03.065`

Gallup, L., Trabia, M., O'Toole, B., Fahmy, Y., 2024. b. Polymers 17 (1), 26.
DOI: `10.3390/polym17010026`

Garzon-Hernandez, S., Garcia-Gonzalez, D., Jérusalem, A., Arias, A., 2020. Design of fdm 3d printed polymers: An experimental-modelling methodology for the prediction of mechanical properties. Materials & Design 188, 108414.
DOI: `10.1016/j.matdes.2019.108414`

Henríquez, C. M. G., Sarabia, M. A., León, M., Hernández, J. R., 2024. Procesos de impresión 3d y materiales para robótica blanda. Revista de plásticos modernos: Ciencia y tecnología de polímeros 127 (802), 3.

Monje, C. A., Relaño, C., Nagua, L. F., Martínez, S., Balaguer, C., 2024. Eslabón para articulación blanda y articulación blanda que comprende dicho eslabón. Patent reference P202030726, Universidad Carlos III de Madrid, 2024-06-19.

Relaño, C., Muñoz, J., Monje, C. A., Martínez, S., González, D., Jan. 2023. Modeling and Control of a Soft Robotic Arm Based on a Fractional Order Control Approach. Fractal and Fractional 7 (1), 8.
DOI: `10.3390/fractalfract7010008`

Rodríguez-Sanz, A., Hernández, C. S., Martínez, S., Monje, C. A., 2025. Influencia de la orientaci´ on del patr´ on de relleno en las propiedades mec´ anicas del tpu de dureza 82a. Simposios del Comité Español de Automática (CEA) 1 (1).
DOI: `10.64117/simposioscea.v1i1.33`

Sánchez, C., González-Menocal, J., Mena, L., Muñoz, J., Monje, C. A., 2026. Workspace expansion in a tendon-driven soft joint through base-rotation mechanism. In: 2026 IEEE 9th International Conference on Soft Robotics (RoboSoft). pp. 1052–1058.
DOI: `10.1109/RoboSoft67810.2026.11522947`

Wang, Y., Xie, Z., Huang, H., Liang, X., 2024. Pioneering healthcare with soft robotic devices: A review. Smart Medicine 3 (1), e20230045.
DOI: `10.1002/SMMD.20230045.`

Yasa, O., Toshimitsu, Y., Michelis, M. Y., Jones, L. S., Filippi, M., Buchner, T., Katzschmann, R. K., 2023. An overview of soft robotics. Annual Review of Control, Robotics, and Autonomous Systems 6 (1), 1–29.
DOI: `10.1146/annurev-control-062322-100607`